

## Single-Pion Production in $\pi^- + p$ Collisions at 2.14 BeV/c\*

VASKEN HAGOPIAN

*Department of Physics, University of Pennsylvania, Philadelphia, Pennsylvania, and University of California, Lawrence Radiation Laboratory, Berkeley, California*

AND

YU-LI PAN

*Department of Physics, University of Pennsylvania, Philadelphia, Pennsylvania*

(Received 8 August 1966)

A bubble-chamber experiment in which the reaction  $\pi^- + p \rightarrow \pi + \pi + N$  was studied at a beam momentum of 2.14 BeV/c yielded 1533 and 2234 events of the final states  $\pi^- \pi^0 p$  and  $\pi^- \pi^+ n$ , respectively. These events are dominated by the formation of the  $\rho$  resonance, which is produced mostly in the forward direction. Both the production and decay angular distributions of the  $\rho^-$  agree very well with the predictions of the one-pion exchange theory modified by absorption effects. The decay angular distribution of the  $\rho^0$  shows the well-known forward-backward asymmetry. This effect is interpretable as the result of the interference between the  $\rho^0$  and an isospin-zero  $s$ -wave  $\pi$ - $\pi$  resonance. The production of the  $\rho^0$ , in addition to its forward peak, shows a weak backward peak. Partial cross sections of various final states are also presented.

### INTRODUCTION

RECENT results from experimental work on single-pion-production processes in pion-nucleon collisions have paved the way to a better understanding of the one-pion-exchange mechanism, especially as modified by absorption effects. So far, the major limitation to such understanding has been the existence of a limited amount of data with which the theoretical predictions can be compared extensively with experimental results.

To obtain more data on the  $\rho$  resonance, we exposed the 20-in. liquid-hydrogen bubble chamber at Brookhaven National Laboratory to a separated beam of  $\pi^-$  mesons. This exposure was a continuation of a similar experiment performed previously at a  $\pi^-$  momentum of 3.00 BeV/c.<sup>1</sup> The beam momentum was selected at 2.14 BeV/c to obtain the maximum partial cross section for  $\rho$  production while keeping the isobar effects to a minimum. This choice of momentum also allowed clear separation between protons and pions by ionization of their tracks.

Below, we present the data on the reactions

$$\pi^- + p \rightarrow \pi^- + \pi^0 + p, \quad (1)$$

$$\pi^- + p \rightarrow \pi^- + \pi^+ + n, \quad (2)$$

in which the most prominent feature is the  $\rho$  resonance decaying into two pions. We have analyzed the events of these reactions in a similar manner as the Penn-Saclay collaboration at beam momenta of 2.75 and 3.00 BeV/c.<sup>2</sup> The results of this and the Penn-Saclay experiment are very similar. To make the data compatible for comparison purposes, we have used the same nota-

\* Work supported in part by the U. S. Atomic Energy Commission.

<sup>1</sup> V. Hagopian and W. Selove, Phys. Rev. Letters **10**, 533 (1963); V. Hagopian, Ph.D. thesis, University of Pennsylvania, 1963 (unpublished).

<sup>2</sup> V. Hagopian, W. Selove, J. Alitti, J. P. Baton, and M. Neveu-René, Phys. Rev. **145**, 1128 (1966). See the references in this paper for other related experiments.

tions throughout. Data from other reactions from this bubble chamber exposure will be presented elsewhere.

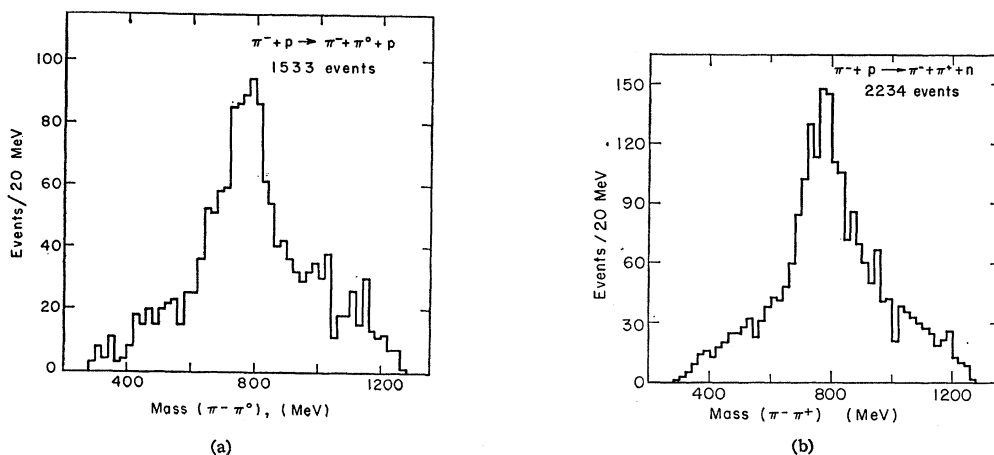
### EXPERIMENTAL METHODS

The BNL 20-in. bubble chamber was exposed to a  $\pi^-$  beam at the alternating gradient synchrotron. We estimated the  $K^-$  and  $\bar{p}$  contamination in the separated  $\pi^-$  beam to be less than 0.01%, and the  $\mu^-$  contamination to be less than 15%. The beam-momentum spread was about  $\pm \frac{1}{2}\%$ . All the film was first scanned for two-prong events (i.e., two charged particles going out from an interaction vertex). About 12% of the film was re-scanned for all interactions, yielding an over-all two-prong scanning efficiency of 90%. The interaction vertex of the events was restricted to a fiducial volume 23 cm long along the beam direction.

About 12 000 events were found and measured in three views on image-plane digitizers with an accuracy of 10  $\mu$  referred to the film. The measured events were reconstructed and kinematically fitted by an IBM 7040 computer using the TRED-KICK programs. These programs were written at Brookhaven National Laboratory and Lawrence Radiation Laboratory and modified by us for our own use.

Most of the events were identified readily by the kinematical fits together with a rough estimate of the ionization of the charged tracks. The other events were identified by measuring the ionization of the ambiguous tracks on the scan tables. Events with ambiguous positively charged tracks constituted less than 0.2% and were of little consequence to our analysis. From the missing-mass calculations, the identities of the neutral particles were determined, and are discussed in the next section.

The final analysis of the events which were identified as either reaction (1) or (2) was done at the Lawrence Radiation Laboratory on an IBM 7094 computer using the SUMX program.

FIG. 1.  $\pi$ - $\pi$  invariant mass: (a)  $\pi^-\pi^0$ , (b)  $\pi^-\pi^+$ .

### CROSS SECTIONS

To obtain the total scattering cross section, we scanned more than 12% of the film for all interactions within the fiducial volume. Our scanning efficiency for the two-charged-prong events during this scan was 99%. Table I contains the results of this scan. The two-prong cross section, 28.7 mb, was obtained by normalizing the total scattering cross section to the value of 35.7 mb obtained by Diddens *et al.*<sup>3</sup> Our partial cross sections for the channels which contribute to the two-prong events were then obtained by normalizing the total two-prong events to a cross section of 28.7 mb. The number of events and the cross section for each channel are also listed in Table I.

When pions scatter elastically off protons at very small angles, the protons receive very little momentum and hence have short range; many of such events are thus missed during the scanning. Care in scanning reduces, but can never remove, this bias. This can be corrected for by looking at the forward diffraction peak, which should approximately fit a straight line on a

semilog plot. To correct for this bias, we have included 600 events in the calculation of the elastic-scattering cross section.

In addition to the requirement that the probability for the reaction (1) kinematical fit be greater than 2%, the selection between reactions (1) and (3) (see Table I) was based on the square of the missing mass. Our choice of 0.08 BeV<sup>2</sup> as the upper limit for reaction (1) caused us to misassign about 7% of the events to reaction (3) and approximately 4% in the opposite direction. Likewise, a 1.2 BeV<sup>2</sup> limit on the square of the missing mass for the reaction (2) misassigned about 4% of the events between reactions (2) and (4).

### PRODUCTION OF SINGLE PIONS

In Figs. 1 and 2, we show the dipion invariant-mass distributions of reactions (1) and (2) for (a) all events, and (b) for events with a  $\Delta^2$  limit of  $12\mu^2$ . Here  $\Delta^2$  is defined as the square of the four-momentum transfer to the nucleon, and  $\mu$  as the mass of the charged pion. As in other experiments in this momentum region, the significant feature is the production of the  $\rho$ . From Fig. 1, we see that in the  $\rho$  mass region the nonresonant background is quite large, but is much smaller in Fig. 2. From Fig. 2, we calculate the background for our  $\rho$  events in the  $\pi$ - $\pi$  mass range of 680 to 840 MeV to be about 20%. Our values for the mass and the width of the  $\rho$ , with and without a  $\Delta^2$  limit, are listed in Table II.

The Chew-Low plots (Fig. 3) show the well-known fact that the production of the  $\rho$  is concentrated at low

TABLE I. Number of events and partial cross sections.

Reaction	Events	Cross section (mb)
0-prong	152	
2-prong	1427	28.7±0.7
4-prong	135	
Strange particles	58	
	1772	35.7±0.25
1= $\pi^-\pi^0p$	1533	3.7±0.2
2= $\pi^-\pi^+n$	2234	5.4±0.3
3= $\pi^-p(m\pi^0)$	1216	2.9±0.2
4= $\pi^-\pi^+n(m\pi^0)$	3082	7.4±0.3
5= $\pi^-p$ (corrected)	3864	9.3±0.4
	11 929	28.7

<sup>3</sup> A. N. Diddens, E. W. Jenkins, T. F. Kycia, and K. F. Riley, Phys. Rev. Letters 10, 262 (1963).

TABLE II. Position and width of the  $\rho$ -mass peaks.

	$\rho^-$		$\rho^0$	
	$E_{\text{peak}}$ (MeV)	$\Gamma$ (MeV)	$E_{\text{peak}}$ (MeV)	$\Gamma$ (MeV)
Events with $\Delta^2 \leq 12\mu^2$	765±5	135±20	770±5	135±20
All events	770±5	130±20	770±5	130±20

FIG. 2.  $\pi\text{-}\pi$  invariant-mass spectra for  $\Delta^2 \leq 12\mu^2$ : (a)  $\pi^-\pi^0$ , (b)  $\pi^-\pi^+$ .

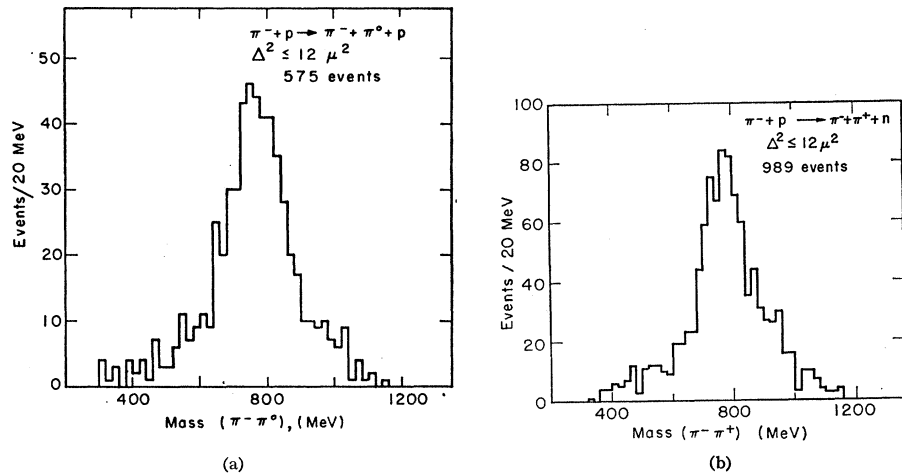
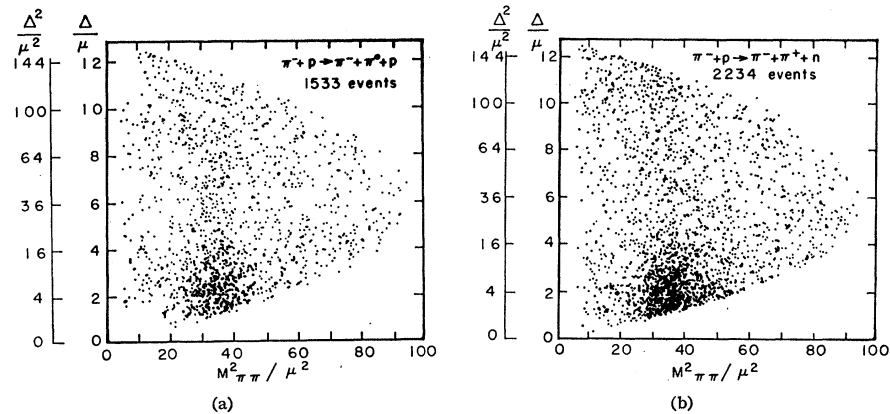


FIG. 3. Chew-Low plots: (a)  $\pi^-\pi^0 p$ , (b)  $\pi^-\pi^+ n$ .

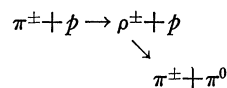


momentum transfers.<sup>4</sup> One can thus increase the ratio of true  $\rho$  events to background by taking only the events in the low-momentum-transfer region. We took a  $\Delta^2$  value of  $12\mu^2$  as the upper limit for this region. This upper limit of  $\mu^2$  is due in part to the fact that the number of  $\rho$ 's produced as a function of  $\Delta^2$  decreases significantly at about this value of  $\Delta^2$  for both  $\rho^-$  and  $\rho^0$ .

Figure 4 gives the Dalitz plot for reactions (1) and (2) for all events. The  $\rho$  bands, which show up at  $135^\circ$ , vary in density along the bands because of the non-uniform decay distribution of the  $\rho$  resonance. In addition to the  $\rho$  resonance, we see some  $N^*(1238)$  isobar production, but this production is reduced to a negligible level when we consider only the low  $\Delta^2$  events (see Fig. 5). We estimate the contamination of  $N^*(1238)$  events in our  $\rho$  sample to be less than 5%.

#### ANALYSIS OF THE $\rho$ RESONANCE

Production and decay of the charged  $\rho$  resonance from the reaction



<sup>4</sup> G. F. Chew and F. E. Low, Phys. Rev. **113**, 1640 (1959).

has been studied extensively using the one-pion-exchange (OPE) model, modified to include absorption effects (OPEA). The agreement of the OPEA calculations performed by Gottfried and Jackson<sup>5</sup> and collaborators<sup>6</sup> with experimental results is excellent in both the production and decay angular distributions. This agreement is, in fact, better than one expects in view of the approximations made in the theory. The  $\rho^-$  data presented in this paper also agree very well with OPEA predictions, thereby strengthening the validity of the model. It should be pointed out that in reactions other than  $\pi + \text{nucleon} \rightarrow \rho + \text{nucleon}$ , the OPEA model is less successful in explaining experimental results.

The  $\rho^0$  resonance produced in  $\pi$ -nucleon collisions has a well-known strong forward-backward asymmetry in its own rest system. This asymmetry in the  $\rho^0$  decay cannot be explained by OPE or OPEA without the addition of a large amount of isospin ( $T$ ) zero  $s$ -wave  $\pi\text{-}\pi$  scattering. Durand and Chiu<sup>7</sup> were able to fit the

<sup>5</sup> K. Gottfried and J. D. Jackson, Nuovo Cimento **34**, 735 (1964). See also J. D. Jackson, Rev. Mod. Phys. **37**, 484 (1965).

<sup>6</sup> J. D. Jackson, J. T. Donohue, K. Gottfried, R. Keyser, and B. E. Y. Svenson, Phys. Rev. **139**, B428 (1965).

<sup>7</sup> L. Durand and Y. T. Chiu, Phys. Rev. Letters **14**, 329 (1965); **14**, 680(E) (1965); L. Durand (private communication).

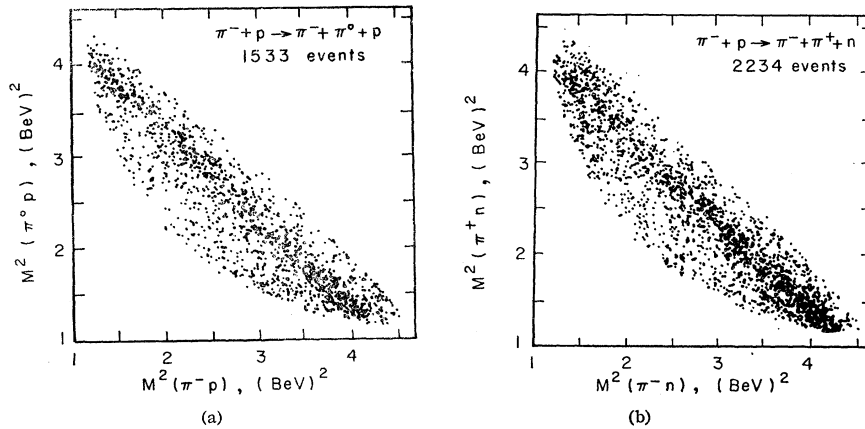


FIG. 4. Dalitz plots: (a)  $\pi^- \pi^0 p$ , (b)  $\pi^- \pi^+ n$ .

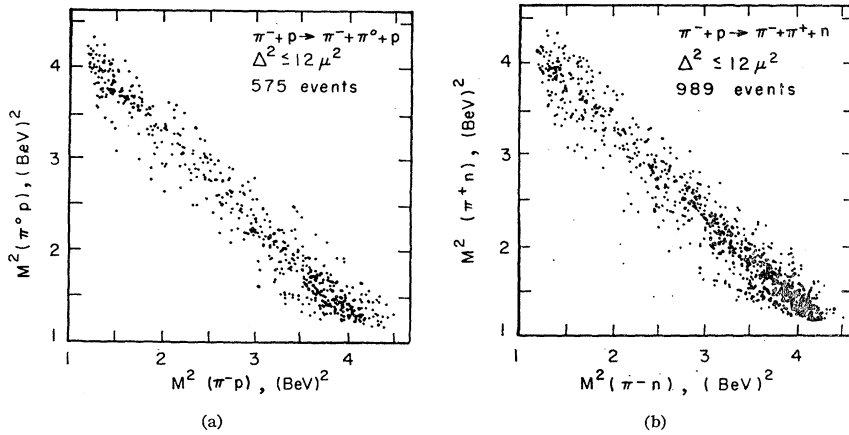


FIG. 5. Dalitz plots for  $\Delta^2 \leq 12\mu^2$ : (a)  $\pi^- \pi^0 p$ , (b)  $\pi^- \pi^+ n$ .

decay distribution of the  $\rho^0$  to OPEA model calculations by adding a resonant  $T=0$   $s$ -wave to the resonant  $p$ -wave. Our data are very similar to those used by Durand and Chiu and so should yield essentially the same results. We make no further attempt to fit our  $\rho^0$  data to the OPEA model.

**A. Production of the  $\rho$  Resonance**

The formation of the  $\rho$  resonance is essentially a peripheral process producing a large concentration of

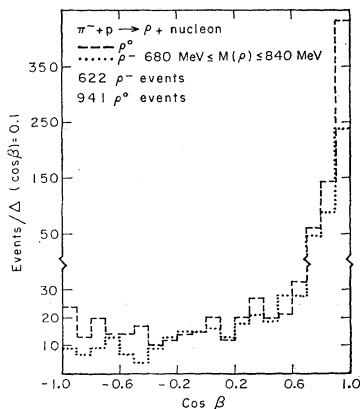


FIG. 6. Production angular distributions for  $\rho^-$  and  $\rho^0$ .

low- $\Delta^2$  events. We define  $\beta$  as the production angle for the dipion in the over-all center-of-mass system.  $\cos\beta$  is linearly related to  $\Delta^2$ ; for a  $\pi^-$  beam momentum of 2.14 BeV/c and a  $\pi-\pi$  invariant mass of 770 MeV, the relationship is

$$\Delta^2/\mu^2 = 1.17 + 65.57(1 - \cos\beta).$$

Figure 6 shows the  $\cos\beta$  distribution of the  $\rho$  events in the mass region  $M(\pi\pi) = 680$  to 840 MeV. The main feature is the extremely forward peak. (Note the change of scale.) Chew and Low predicted this forward peak

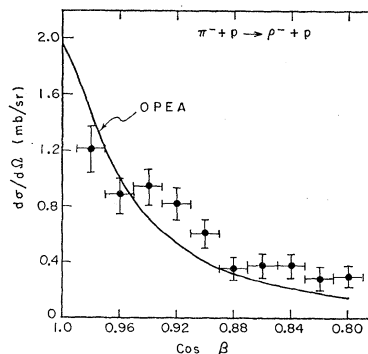


FIG. 7. Differential cross section for  $\rho^-$  production. The smooth curve is the theoretical prediction calculated by Jackson (Ref. 8).

FIG. 8. Four-momentum transfer  $\Delta$  versus  $\cos\theta$ : (a)  $\rho^-$ , (b)  $\rho^0$  ( $\Delta$  is the magnitude of the four-momentum transfer to the nucleon and  $\theta$  is the decay scattering angle in the final dipion rest system).

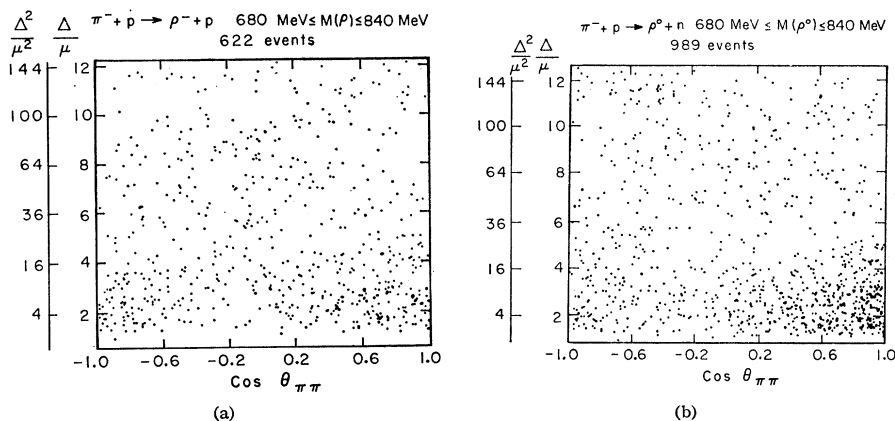
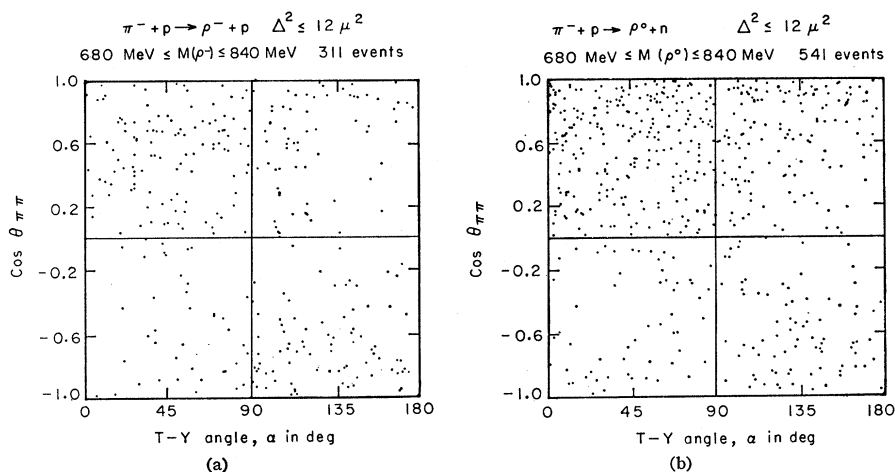


FIG. 9. Decay angular distribution:  $\cos\theta$  versus Treiman-Yag<sup>2</sup> angle  $\alpha$  for events with  $\Delta^2 \leq 12\mu^2$  (a)  $\rho^-$ , (b)  $\rho^0$ .



by assuming the OPE model for  $\pi$ - $\pi$  scattering.<sup>4</sup> But when the  $\rho$  is considered to be a  $p$ -wave  $\pi$ - $\pi$  scattering resonance, the OPE model predicts the wrong magnitudes for both the  $\rho$  partial cross section and the shape of  $d\sigma/d\Delta^2$ . The OPE cross-section value prediction is about twice the experimental value. These discrepancies are removed when the OPE is modified with absorption effects. Figure 7 shows the forward peak of the  $\rho^-$  together with the prediction of OPEA calculated by Jackson.<sup>8</sup> The error bars are statistical and no corrections have been made for biases that exist for  $\cos\beta \geq 0.98$ . The agreement of the theoretical predictions with the experimental values is good. The  $\rho^0$  distribution has not been checked against OPEA because of the complications produced by the  $s$ -wave.

In addition to the forward peaks of the  $\rho$ 's, the  $\rho^0$  has a small backward peak, but the  $\rho^-$  has none (see Fig. 6). This behavior, which was also observed in the Penn-Saclay data,<sup>2</sup> can be explained in terms of an exchange of a baryon. The backward  $\rho^0$  peak needs the exchange of a proton, whereas the backward  $\rho^-$  events need the exchange of a doubly charged baryon, such as

the  $N^*(1238)$ . This behavior is similar to the backward peaks of elastic  $\pi$ -nucleon scatterings where the doubly charged baryon exchanges are much weaker than singly charged nucleon exchanges.<sup>9</sup>

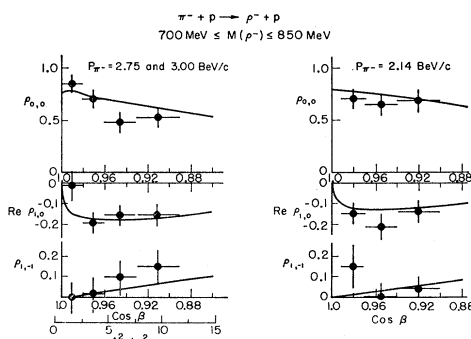


FIG. 10. Spin-density matrix elements for the  $\rho^-$ . The smooth curves are the theoretical predictions of OPEA calculated by Jackson (Ref. 8). The results of the Penn-Saclay data (Ref. 2) at 2.75 and 3.00 BeV/c are included for comparison.

<sup>8</sup> J. D. Jackson (private communication).

<sup>9</sup> For information on elastic scattering see J. Orear *et al.*, Phys. Rev. Letters **15**, 309 (1965); **15**, 313 (1965); H. Brody *et al.*, Phys. Rev. Letters **16**, 828 (1966).

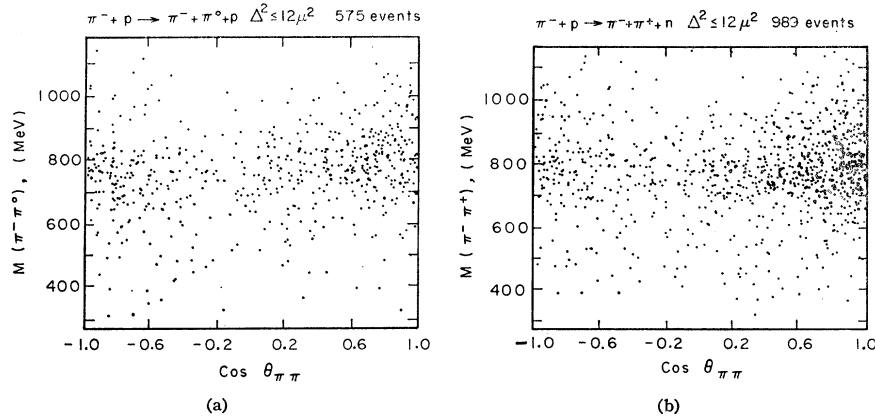


FIG. 11.  $\pi\pi$  invariant mass versus  $\cos\theta$  for  $\Delta^2 \leq 12\mu^2$ : (a)  $\pi^-\pi^0$ , (b)  $\pi^-\pi^+$ .

### B. Decay Angular Distributions of the $\rho$ Resonance

To describe the decay angular distributions of the  $\rho$  resonance, we need to define two angles: (a)  $\theta$ , the  $\pi^-$  polar “scattering angle” defined in the final dipion rest system, and (b)  $\alpha$ , the Treiman-Yang angle, or azimuthal angle in the final dipion rest system defined by

$$\cos\alpha = \mathbf{n}_{21} \cdot \mathbf{n}_{14},$$

where  $\mathbf{n}_{21} = \mathbf{p}_2 \times \mathbf{p}_1 / |\mathbf{p}_2 \times \mathbf{p}_1|$  and  $\mathbf{n}_{14} = \mathbf{p}_1 \times \mathbf{p}_4 / |\mathbf{p}_1 \times \mathbf{p}_4|$  with  $\mathbf{p}_1$ ,  $\mathbf{p}_2$ , and  $\mathbf{p}_4$  equal, respectively, to the three-momentum of the incoming  $\pi^-$ , the outgoing  $\pi^-$ , and the outgoing nucleon.

For a pure  $p$ -wave  $\pi$ - $\pi$  scattering resonance with no background or other effects, such as absorption, the decay angular distribution should be proportional to  $\cos^2\theta$ , and should be isotropic for the Treiman-Yang angle  $\alpha$ . Figure 8 shows  $\cos\theta$  versus  $\Delta$  for the  $\rho$  events. Even though the background increases with  $\Delta^2$ , the angular distribution changes faster than warranted by background. For  $\rho^-$ , the distribution is predominantly that of  $\cos^2\theta$  for events with  $\Delta^2$  less than  $4\mu^2$ , and becomes more isotropic for higher values of  $\Delta^2$ . The  $\rho^0$  decay angular distribution also changes with  $\Delta^2$  but keeps its forward-backward asymmetry to much higher values.

The other feature of the decay distribution is the diagonal effects in the  $\theta$ - $\alpha$  plots shown in Fig. 9. Both of these non-OPE features can be explained on the basis of the OPEA model. In fact, OPEA is the only known model that predicts correctly the  $\theta$ - $\alpha$  correlation terms. Since the  $\rho^0$  is complicated by the presence of an  $s$  wave, we limit our quantitative comparison of the OPEA with the experimental data to the  $\rho^-$  resonance. To investigate further these effects, we examine the decay angular distributions of a  $p$ -wave resonance in terms of density matrix elements  $\rho_{mm'}$ . (The notation is the same as used by Gottfried *et al.*<sup>5</sup>)

$$W(\theta, \alpha) = \frac{3}{4} [\rho_{00} \cos^2\theta + \frac{1}{2}(1 - \rho_{00}) \sin^2\theta - \rho_{1,-1} \sin^2\theta \cos 2\alpha - \sqrt{2} \operatorname{Re} \rho_{10} \sin 2\theta \cos \alpha].$$

From the  $\rho^-$  data, we calculated the  $\rho_{mm'}$  elements for several regions of  $\cos\beta$  by the maximum likelihood

method. Figure 10 shows the results together with the theoretical predictions calculated for us by Jackson.<sup>8</sup> For comparison, we also show the results from the Penn-Saclay data.<sup>2</sup> The error bars are statistical, and no corrections have been made for either biases or background. The agreement of OPEA with the experimental results is excellent. For  $\rho^-$  events with  $\cos\beta > 0.98$ , we have an experimental bias mentioned before and so the values of  $\rho_{mm'}$  for  $\cos\beta > 0.98$  are not necessarily correct. It should also be mentioned that as  $\cos\beta$  decreases to 0.9 (i.e.,  $\Delta^2$  increases to  $8\mu^2$ ), the nonresonant background increases.

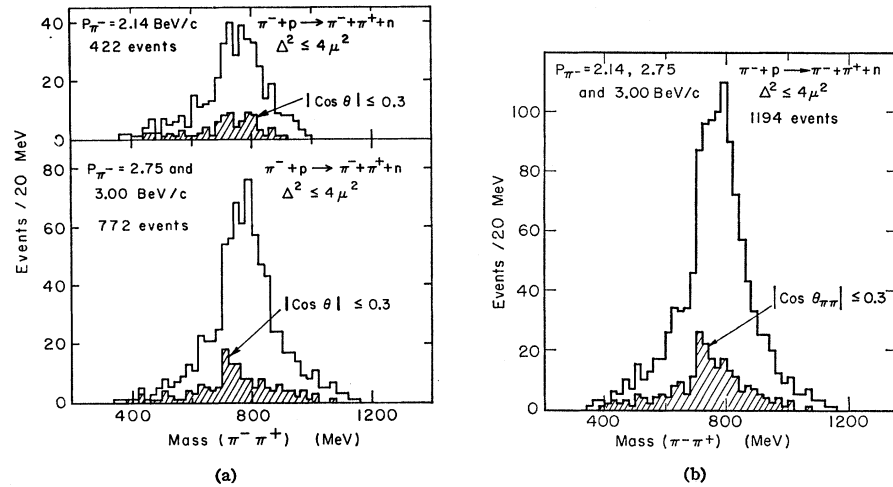
Since the  $\rho^0$  decay distributions are complicated by the possible presence of  $s$ -wave and some  $d$ -wave background, we do not attempt any quantitative determinations. Others have calculated the density matrix elements for the  $\rho^0$ .<sup>10</sup> We point out that both the change of  $\cos\theta$  distribution towards isotropy with increasing  $\Delta^2$ , and the  $\theta$ - $\alpha$  diagonal effect are qualitatively in agreement with OPEA.

### FINAL REMARKS

In Fig. 11, we show the dipion mass versus  $\cos\theta$  for reactions (1) and (2) with  $\Delta^2 \leq 12\mu^2$ . We note that, for the reaction (1) events, the  $\cos\theta$  plot is more populated in the backward direction for  $M(\pi\pi)$  below the  $\rho$  mass region. The density of events becomes more symmetrical in the  $\rho$  mass region. Above the  $\rho$  mass region, the events are concentrated almost entirely in the forward direction. This effect can be reproduced by adding a  $T=2$   $s$ -wave background with a negative phase shift of approximately  $10^\circ$  to the  $p$ -wave resonance. In contrast, the reaction (2) events are strongly populated in the forward direction for most of the dipion mass range shown in Fig. 11. The density of events along  $\cos\theta$  becomes uniform only at low dipion masses. This result can be simulated by including a large positive

<sup>10</sup> I. Derado, V. P. Kenny, J. A. Poirier, and W. D. Shepard, Phys. Rev. Letters 14, 872 (1965); E. West, J. H. Boyd, A. R. Erwin, and W. D. Walker, Phys. Rev. 149, 1089 (1966).

FIG. 12.  $\pi^- \pi^+$  invariant mass for  $\Delta^2 \leq 4\mu^2$  with and without  $|\cos\theta| \leq 0.3$ : (a) the 2.14 BeV/c and the 2.75+3.00 BeV/c experiments, (b) the sum of 2.14, 2.75, and 3.00 BeV/c experiments.



phase shift in the  $T=0$   $s$ -wave  $\pi\pi$  scattering.<sup>11</sup> With the limited number of events available at present and the uncertainties in the theory, it is not possible to determine the sign of the  $s$ -wave phase shift when the  $p$  wave is near resonance. However, the sign of the  $s$ -wave phase shift can be determined when the  $p$  wave is not near resonance. Jacobs and Selove, who studied this problem, estimated the phase shift to be in the range  $+35^\circ$  to  $+55^\circ$ , in the 400- to 500-MeV interval.<sup>11</sup> Durand and Chiu<sup>7</sup> made a detailed calculation on a model in which the existence of an  $s$ -wave resonance was assumed, and obtained good agreement with the experimental data when the mass of this resonance is about 730 MeV and the width about 90 MeV. There is also some experimental indication of the existence of such a resonance.<sup>12,13</sup>

In order to investigate the possible existence of this  $s$ -wave resonance, we have used the same technique as the Penn-Saclay-Bologna collaboration.<sup>13</sup> Since our data

<sup>11</sup> L. D. Jacobs and W. Selove, Phys. Rev. Letters **16**, 669 (1966).

<sup>12</sup> M. Feldman *et al.*, Phys. Rev. Letters **14**, 869 (1965).

<sup>13</sup> V. Hagopian *et al.*, *ibid.* **14**, 1077 (1965).

alone are too meager to add anything significant to the present knowledge, we also combined our data with the data of Ref. 13. Figure 12(a) shows separately the dipion mass plots with and without the  $\cos\theta$  limits for our present data and the Penn-Saclay-Bologna collaboration. The sum of the two experiments is shown in Fig. 12(b). The shift of the mass peak to a lower value is clear. We note, however, that other experimenters have not observed this effect.<sup>14</sup>

#### ACKNOWLEDGMENTS

We are indebted to Professor W. Selove for his interest, help, and support throughout this experiment. The help of Sharon Hagopian, Richard Van Berg, Robert Ehrlich, Jim Niederer, and Roy Marshall in various stages of this experiment was invaluable. We are grateful to Professor J. D. Jackson for the calculations of the OPEA model. We are grateful also for the excellent support of the AGS staff as well as the BNL 20-in. bubble chamber crew.

<sup>14</sup> H. O. Cohn *et al.*, Phys. Rev. Letters **15**, 906 (1965); E. West *et al.* (Ref. 10); L. D. Jacobs (private communication).